Environment and Planning A, 1989, volume 21, pages 1447 – 1472

Urban growth and form: scaling, fractal geometry, and diffusion-limited aggregation

M Batty, P Longley
Department of Town Planning, University of Wales College of Cardiff, PO Box 906, Cardiff CF1 3YN, Wales

S Fotheringham
National Center for Geographic Information and Analysis, and Department of Geography, State University of New York at Buffalo, Buffalo, NY 14260, USA
Received 6 October 1988

Abstract. In this paper, we propose a model of growth and form in which the processes of growth are intimately linked to the resulting geometry of the system. The model, first developed by Witten and Sander and referred to as the diffusion-limited aggregation or DLA model, generates highly ramified tree-like clusters of particles, or populations, with evident self-similarity about a fixed point. The extent to which such clusters fill space is measured by their fractal dimension which is estimated from scaling relationships linking population and density to distances within the cluster. We suggest that this model provides a suitable baseline for the development of models of urban structure and density which manifest similar scaling properties. A typical DLA simulation is presented and a variety of measures of its structure and dynamics are developed. These same measures are then applied to the urban growth and form of Taunton, a small market town in South West England, and important similarities and differences with the DLA simulation are discussed. We suggest there is much potential in extending analogies between DLA and urban form, and we also suggest future research directions involving variants of DLA and better measures of urban density.

1 Introduction

Contemporary models of urban structure and dynamics are based on elaborate theoretical relationships linking location, density, and urban evolution, but they rarely address specific issues of urban form. Models are postulated at more aggregate levels than those involving the geometry of urban development, and although such models are often consistent with urban form, their processes and mechanisms are largely independent of geometrical considerations (Bertuglia et al, 1987). Theoretical models of urban systems, such as those based on urban economics, depend upon certain assumptions regarding form, but such models invariably define away form in grossly simplified treatments of urban space (Thrall, 1987). In short, it has proved extremely difficult to build models linking statics and dynamics to particular forms: whenever form is relevant, it is incorporated as an assumption of analysis, a given, never a consequence of the processes at work. Consequently, research into urban form has remained apart from the mainstream of theorising in urban studies, and such work that there is has been considered idiosyncratic, sometimes falling into disrepute.

During the last decade, however, there have been major developments in the science of form, particularly within physics and mathematics. This concern is based on the need to link physical processes of growth to form, but it has also been aided by the study of natural forms based on the emergence of a geometry of the irregular. The visualisation and mathematical description of such forms has been spurred on by developments in computer graphics, and great strides have been made in visualisation by using the mathematics of fragmented or 'broken' structures: fractals (Mandelbrot, 1983). Developments range from simple but realistic simulations of natural forms, such as landscapes, which largely involve 'adding'

fractal ideas to more conventional simulations, to much deeper theoretical ideas involving the way physical processes generate fractal structures.

The most complete examples of this new approach to modelling form have developed in the physics of critical phenomena, particularly involving the aggregation and growth of fine particles. Since the early 1980s, computer simulation models have been used to generate forms which are visually similar to a variety of particle clusters, which also manifest spatial self-similarity across a wide range of scales, and whose structure is subject to scaling laws consistent with ideas in fractal geometry. The clearest, most articulate examples can be generated by a process of diffusion about a seed particle, such diffusion taking place on a regular lattice which embodies the seed. These models, first suggested by Witten and Sander (1981; 1983), are collectively known as diffusion-limited aggregation or DLA models. The structures generated are familiar tree-like forms or dendrites, grown from the seed, manifesting self-similarity of form across several scales, and whose properties of scaling suggest that they are fractals.

The great power of these techniques is that they link growth to specific geometrical forms. They can be easily generalised to other forms such as those with the characteristics of percolation clusters; and more importantly, they are consistent with the sorts of scaling found in the physics of critical phenomena, particularly in structures which are far-from-equilibrium (Feder, 1988). These ideas have excited so much interest in the last seven years since they were first proposed that it has prompted the physicist Kadanoff (1986, page 6) to say: "*Physical Review Letters* complains that every third submission seems to concern fractals in some way or another". Between 1981 and 1986 the index to *Physical Review*: *Letters A*, *B*, *C*, and *D* lists 120 papers on DLA in these journals alone. There are many other papers in other physics journals and conference proceedings, and there are now several books on the subject (see for example, Feder, 1988; Jullien and Botet, 1987; Stanley and Ostrowsky, 1986).

In this paper we intend to demonstrate how these ideas might be useful in simulating urban structure, and in particular in demonstrating how growth and form can be inextricably linked. We will proceed using the time-honoured method of analogy (Wilson, 1969). To anticipate our conclusions, there is no perfect correspondence between theoretical DLA simulations and the empirical urban structure based on the town of Taunton which we use as a basis for comparison. Nevertheless, the similarities are strong, and give us confidence that this approach has great potential in urban simulation, a potential which we will explore further in future papers. However, what the approach does suggest is that traditional ways of measuring urban structure, particularly urban population densities, are extremely limited. The DLA approach suggests we must define and measure densities much more accurately, having recourse not to general urban concepts such as the density of developed areas but to the actual geometry of location: populations measured as point locations, not as areas or volumes. This has important implications for models of urban density and previous quantitative measures of urban population density. If this is the only consequence of this approach, it will have been worthwhile in that it will demonstrate how woolly the existing concept of urban density is, and how necessary it is to relate such densities to particular forms.

We will begin by sketching key relationships between the development of systems which diffuse around a central point, particularly emphasising their analogy to city systems. We will postulate some simple but profound scaling relationships which imply structures which are statistically fractal. DLA is introduced as one such model which generates such forms. Our concern will be twofold: first, to measure spatial clusters in appropriate ways which enable scaling relationships to be

estimated, and, second, to look at the dynamics involved in the growth of such clusters in both space and time. We will then be in a position to demonstrate how DLA can generate such structures, and we will present a framework for estimating model relationships in both space and time. At this point we are able to demonstrate how the framework can be applied to a real system. We will apply it to the town of Taunton, but our emphasis will be entirely in terms of a static comparison because the history of the town's urban dynamics is not available to us. The comparisons we make between DLA and Taunton are close statistically, but we need a much finer measurement of density to be able to compare rigorously the two forms. This, as well as the development of variants of the DLA model, will help us to define directions for future research, which we will present in our conclusions.

2 Scaling laws of urban form

Imagine the simplest process in which a city might grow from some central point or site. Through time, the city grows by new individuals locating next to or near individuals who have already clustered about the central point. If the city were to grow irreversibly and if individuals were to occupy every available space adjacent to the growing cluster, the area of the city would expand in proportion to the square of the radius of the cluster. However, it is unlikely that all available space would be occupied as the city grows. Other land-uses are required, some space always remains vacant owing to physical obstacles to development, and so on. In real cities, the population is never stable, for individuals move within the city and occupied sites become unoccupied. For the moment, we will assume that once an individual locates, the location remains occupied; this type of irreversibility is still consistent with a process in which individuals can move within the city, although it assumes that once physical locations are occupied they remain so.

The essential variables describing this growth are $N(r)$, the cumulative number of occupied sites at radius r from the centre, and $A(r)$, the total area of all sites both occupied and unoccupied at radius r from the centre. Both $N(r)$ and $A(r)$ increase with r and can be specified as

$$N(r) \propto r^D , \tag{1}$$

$$A(r) \propto r^d , \tag{2}$$

where D is the parameter or scaling exponent which scales population with distance, and d is the parameter which scales area with distance. We have explicitly assumed d to be the dimension of area, that is $d = 2$, although we will continue to refer to this dimension as d because our equations can then be generalised to any dimension.

The obvious variable of interest is the density $\rho(r)$, which from equations (1) and (2) is defined as

$$\rho(r) = \frac{N(r)}{A(r)} \propto r^{D-d} . \tag{3}$$

The change in population and area, the first derivatives of equations (1) and (2) with respect to r, are given as

$$\frac{dN(r)}{dr} \propto r^{D-1} , \tag{4}$$

and

$$\frac{dA(r)}{dr} \propto r^{d-1} , \tag{5}$$

and the ratio of equations (4) and (5) also defines the density at the margin as

$$\frac{dN(r)}{dr} \Big/ \frac{dA(r)}{dr} = \frac{dN(r)}{dA(r)} \propto r^{D-d} . \tag{6}$$

Finally, the change in density with respect to distance is given as

$$\frac{d\rho(r)}{dr} \propto r^{D-d-1} , \tag{7}$$

and higher derivatives of equation (7) can be taken if required.

These relationships in equations (1) to (7) are only of substantive interest if values are specified for D and d. First, the physical dimension d could relate to a line, area, or volume. In fact, we have assumed $d = 2$, which we will use throughout this paper, but it is possible to develop the analysis for urban systems with $d = 3$ if the population were to be modelled in three dimensions. From our earlier argument, we assumed $1 < D < 2$, that is, that the population does not occupy the entire space $A(r)$ which would imply $D = 2$ and a uniform density, nor does the population simply vary with the radius, r, for this would imply a linear city.

From equations (1) to (7), we will develop the following four relationships assuming that $d = 2$. Then

$$N(r) \propto r^{\beta_1} , \qquad \beta_1 = D , \tag{8}$$

$$\frac{dN(r)}{dr} \propto r^{\beta_2} , \qquad \beta_2 = D-1 , \tag{9}$$

$$\rho(r) \propto r^{\beta_3} , \qquad \beta_3 = D-2 , \tag{10}$$

and

$$\frac{dN(r)}{dA(r)} \propto r^{\beta_4} , \qquad \beta_4 = D-2 . \tag{11}$$

If we assume $1 < D < 2$ then β_1 and β_2 in equations (8) and (9) are positive, and the exponent on density, β_3, in equation (10) is negative, hence consistent with traditional urban density theory and observation (Mills, 1970). The exponent on marginal density, β_4, is also negative and in theory should equal β_3. These β parameters can be estimated by using ordinary least-squares regression on the logarithmic transforms of equations (8) to (11), and represent different ways of calculating the scaling parameter, D. A fifth estimate of D could be derived from equation (7) where the parameter is $D-3$. However, the relationship is negative and cannot be easily estimated by regression. We have thus excluded this from our subsequent analysis.

The above relationships describe how the population of a city or the particles in a cluster fill space, and, as we have argued, it is reasonable to assume that the density of the city or cluster falls at increasing radial distance, r, from the centre. This is of course borne out by casual observation, which suggests D cannot be as large as 2 but is certainly greater than 1. There is another way of considering how population fills space. Let us assume that populations can be linked by a continuous line. If every population point on a lattice were occupied, there are well-known curves which can link such points and seem to fill space. However, it is always possible to find a continuous curve which links less than all the points on a lattice (assuming some are unoccupied). Such a curve is clearly longer than the diameter of the city, but not as long as the space-filling curve linking every lattice point. It is well-known that such a curve has a dimension greater than the line ($D = 1$) but less than the area ($D = 2$), and this noninteger or fraction of the Euclidean

dimension is called the fractal dimension. As such it is a measure of the extent to which space is filled, playing a central role in the development of fractal geometry (Feder, 1988).

Scaling relationships such as these have been used throughout the development of social physics. In one sense, we have always been working with fractals and fractal dimensions, but the new framework provides links between these relationships and the underlying geometry of the system, which hitherto has eluded us. We have already noted the consistency between urban density theory and densities as given by equations (10) and (11), but considerable work has also been done on relationships between population and area. From equations (1) and (2) it is clear that area could be derived from population as $A(r) = N(r)^{\phi}$. The parameter ϕ is thus d/D, which must be greater than unity. Area obviously grows at a faster rate than population with respect to increasing radial distance, or alternatively the relative change in area is always greater than the relative change in population by a factor of $\phi(= d/D)$. These types of relationship are allometric and have been extensively studied with respect to the growth of cities (Dutton, 1973; Nordbeck, 1971; Woldenburg, 1973). In the development of urban allometry there has been little attempt to link these scaling coefficients to urban form, and most of the analysis has been with respect to the growth of different cities through time, not individual cities across space. Nevertheless, there are connections here between fractal geometry and urban allometry, which will be explored in later papers.

There is also a connection between the fractal dimension, D, in this context and the exponents in gravitational and potential models of spatial interaction (Stewart and Warntz, 1958). From the approach developed here, we would argue that the value of the exponent in such gravity models is a consequence of the form of the system, rather than of any noise in the data (Curry, 1972). These links will also be explored in future papers, but it is worth noting that the ideas developed here might represent a new variety of social physics, a "post modern" social physics as one commentator has already referred to it (Woolley, 1988). In this blend of physics, growth and form are inextricably linked.

3 The process of diffusion-limited aggregation

The above scaling relations can be estimated for any spatial system of individual objects in which central points can be identified; as such, these relationships are independent of any particular spatial form. In this paper, however, we will introduce a particular spatial form which results from a growth process of constrained diffusion known as diffusion-limited aggregation. This will represent our baseline model in which we will make comparisons with observable urban growth. It is necessary now that we introduce the DLA model. To this end we will follow the terminology of the field and refer to the irreducible objects of the system as 'particles'.

Consider a bounded circular region with a single seed particle fixed at its centre. New particles are launched from points far away from the seed, from a circular boundary which is at least three times the radius of the cluster grown so far. These particles are launched from random points on this boundary one at a time. When a launch occurs, the particle begins a random walk, usually on a regular lattice, often square, which is centred over the seed particle, the particle moving only one lattice step at a time. Two states can occur: if the particle moves outside the boundary circle, it is 'killed', or destroyed; if it approaches the cluster and is within a neighbourhood, usually one lattice step, of a particle already fixed, it sticks to the particle, its walk is terminated, and the cluster is extended. If either of these cases occur, another particle is launched, and the process of 'walking' on the lattice begins again. The process only terminates once a size threshold is

reached, such as that based on a fixed cluster size in terms of the number of particles, or once a maximum cluster radius or cluster span is attained.

The form which results is dendritic, with tentacles extending from the seed particle, growth proceeding in a tree-like fashion. It is not immediately obvious why this is so, but a little thought reveals that when a particle sticks to another, the probability of more particles sticking in that neighbourhood is much increased. Ribbons of particles begin to form around the centre of the cluster, making it ever more likely that new particles will stick to the tips of existing dendrites which effectively screen the fissures between the emerging tentacles from receiving further particles (Sander, 1987). The resulting form [which can be seen in abstract in figure 1(a) and in simulation in figure 1(b) (see section 6)] is clearly fractal in that the dendrites making up the cluster appear to be similar at every scale.

The association between particle clusters and fractal geometry goes back to a paper by Forrest and Witten (1979), but the original model was suggested by Witten and Sander (1981; 1983). Its subsequent application to and estimation of different particle clusters was motivated by its clear visual similarity to many naturally occurring forms. The diffusion process itself has high generality in that it is consistent with the Laplace equation which applies to many physical systems. Other models such as those simulating such phenomena as dielectric breakdown (Neimeyer et al, 1984; Satpathy, 1986) and viscous fingering (Nittmann et al, 1985) are also consistent with DLA. As indicated in our introduction, there have been extensive explorations of the DLA model. Meakin (1983a; 1983b; 1986a; 1986b) has explored a variety of simulations with dimensions ranging from $d = 2$ to $d = 6$, and with particle systems of varying sizes. Changes to the probabilities of sticking have been investigated as well as constraints on the direction of the random walks, all illustrating the robustness of the model.

Apart from the highly characteristic form generated by the model, several independent researchers have concluded that D is approximately equal to 1.71 for the DLA model. This dimension hardly changes when the sticking probability is relaxed, although there is still considerable argument concerning the universality of the scaling exponent (Meakin, 1986c). There is some work which suggests that the shape of the underlying lattice has an effect on the simulation (Meakin, 1985; Turkevich and Scher, 1985). Attempts at generating a mean field theory for the model by Muthukumar (1983) have led to a prediction that D is equal to $(d^2+1)/(d+1)$, which for a two-dimensional system gives D equal to $5/3$ (1.66) and for a three-dimensional system gives D equal to $5/2$ (2.5); both of these values are consistent with the simulations. But as yet there is no general consensus concerning these issues. The most complete review of this enormous body of work is contained in the book by Jullien and Botet (1987).

At this stage we must attempt a preliminary justification for the choice of DLA as a baseline model for our urban simulations. On a casual level, many rapidly growing cities during the nineteenth and twentieth centuries appear to be structured along transportation routes radiating from the central business district. Similar dendrites incorporating the same pattern are associated with smaller commercial centres within the city, which are also structured in a fairly clear hierarchy based on several orders of transport route. We have a problem in saying much more than this because of the way in which urban form is traditionally characterised and measured. Much of urban morphology is predicated in terms of land-use patterns and physical structures, which do not map easily onto the density and distribution of population. Urban population densities are usually defined across large census-tracts rather than in terms of the actual physical location of the population. Indeed, there is some speculation in urban allometry that urban populations should be

conceptualised in three not two dimensions (Dutton, 1973), but there has been no investigation of how such densities are reflected in the geometry of urban form. Thus, it is not surprising that the sorts of form which are characteristic of DLA are not manifest in the data on which urban population density models have been developed. In short, a clearer view of how processes of growth give rise to particular urban geometries, such as those seen in DLA, would provide a new approach to the measuring of urban densities. It is still very much an open question as to whether the dendritic structures of DLA are highly correlated with the geometrical characteristics of urban growth. Such verification must await better data.

The other major issue relates to the process by which DLA occurs. Clearly, urban growth is based on a kind of diffusion which leads to cities growing at their edges. But the process of random wandering necessary to DLA cannot be given any physical meaning in the behaviour patterns of individuals locating in cities. The random walking could be thought of as a proxy for the process of spatial search which does not normally take place physically, but this analogy is not worthy of extensive research. Moreover, cities are not irreversible in the sense in which DLA clusters are. There is substantial mobility among any urban population owing to changes in life style, to economic competition, and such like, which change occupancies in the physical stock of buildings in any city. We fully recognise these issues and intend to broach them in future work. However, in this paper we consider it necessary to begin with the simplest DLA model and only in future work will we adapt this to the peculiarities of urban growth. The only work we are aware of which has proceeded in a not too dissimilar fashion is Lovejoy et al's (1986) project in which they examined the global pattern of meteorological stations with respect to their coverage of the Earth's weather. In this, they used the relationships defined in equations (8) to (11), and estimated a fractal dimension, D, approximately equal to 1.75, which indicates that any global phenomena with a dimension of D less than 0.25 could not be detected by the existing network of stations.

4 Statistical measurement of diffusion-limited aggregation

In estimating the dimension of any structure which can be described as a cluster of particles around a central seed, such as DLA clusters, we will assume that there is a total of N particles, each of which occupies a unique location on a regular lattice. The distance from any particle, l, to any other particle, k, is given as r. The range of l and k is 1 to N; these index numbers are consistently ordered around the central seed-site on the lattice, where l and k equal 1. Suppose particle k is at distance r from a particle l, then let us define

$$p_{lk}(r) \begin{cases} = 1 \text{ if a particle } l \text{ occupies a lattice point,} \\ = 0 \text{ otherwise.} \end{cases}$$

We will now present two sets of measures: first, those based on a location around the seed-site $k = 1$, and, second, those based on locations around every occupied site, which are formed as averages. We refer to the first as one-point measures, and to the second set as two-point measures.

First, then, for the one-point measures, the number of particles at a given distance r from the seed-site is given as $n_1(r)$, or $n(r)$:

$$n(r) = n_1(r) = \sum_l p_{l1}(r), \tag{12}$$

where the summation in equation (12) is over all those particles l which are at distance r (or in distance band r) from the seed, k (= 1). Note that we can suppress the index $k = 1$ in subsequent notation because all the one-point measures introduced are relative to this seed-site. The cumulative number of particles at all distances up to a radius R is given as

$$\mathrm{N}(R) = \sum_{r=1}^{R} \mathrm{n}(r) , \tag{13}$$

and the number of particles at distance R or in a band at R is

$$\Delta\mathrm{N}(R) = \mathrm{N}(R) - \mathrm{N}(R-1) = \mathrm{n}(R) . \tag{14}$$

Note that $N(0)$ is not defined. $\mathrm{N}(R)$ is equivalent to $\mathrm{N}(r)$ in equations (1) and (8), and $\Delta\mathrm{N}(R)$ can be used as $\mathrm{dN}(r)/\mathrm{d}r$ in equations (4) and (9), where the distance bands $r = 1, 2, \ldots, R$ are equal in all cases.

To measure density we must count all lattice points, occupied or unoccupied, around each point $\mathrm{p}_{l1}(r)$ associated with r, and these are defined as $\mathrm{s}(r)$. The total number of such points up to distance R is given as

$$\mathrm{S}(R) = \sum_{r=1}^{R} \mathrm{s}(r) , \tag{15}$$

and the density of particles associated with all distances up to R is thus

$$\rho(R) = \frac{\mathrm{N}(R)}{\mathrm{S}(R)} = \left[\sum_{r=1}^{R} \mathrm{n}(r)\right] \Big/ \sum_{r=1}^{R} \mathrm{s}(r) . \tag{16}$$

Two measures of the change in density can be computed. First, from equation (16):

$$\Delta\rho(R) = \rho(R) - \rho(R-1) = \frac{\mathrm{N}(R)}{\mathrm{S}(R)} - \frac{\mathrm{N}(R-1)}{\mathrm{S}(R-1)} , \tag{17}$$

and, second,

$$\mathrm{Q}(R) = \frac{\Delta\mathrm{N}(R)}{\Delta\mathrm{S}(R)} = \left[\sum_{r=1}^{R} \mathrm{n}(r) - \sum_{r=1}^{R-1} \mathrm{n}(r)\right] \Big/ \left[\sum_{r=1}^{R} \mathrm{s}(r) - \sum_{r=1}^{R-1} \mathrm{s}(r)\right] = \frac{\mathrm{n}(R)}{\mathrm{s}(R)} , \tag{18}$$

from equations (14) and (15). Equation (16), the cumulative (average) density, is equivalent to equations (3) and (10), equation (17) is equivalent to equation (7), and equation (18) to (6) and (11). As noted previously we will not use equation (17), and in the subsequent analysis, equations (13), (14), (16) and (18) will be used as approximations to equations (8), (9), (10), and (11), respectively.

So far, these measures are all specified in terms of the radius r, or R, about a central point, the seed-point at the centre of the lattice. It is possible, indeed appropriate owing to the self-similarity of DLA clusters, to compute the measures as averages around all N particles in the system. In analogy to equation (12), we first compute the number of particles $\mathrm{n}_k(r)$ at distance r from *any* lattice point containing a particle, k, as

$$\mathrm{n}_k(r) = \sum_{l} \mathrm{p}_{lk}(\mathrm{r}) . \tag{19}$$

The average of all particles at distance r from one another is then given as

$$\bar{\mathrm{n}}(r) = \frac{1}{N} \sum_{k=1}^{N} \mathrm{n}_k(r) = \frac{1}{N} \sum_{k=1}^{N} \sum_{l} \mathrm{p}_{lk}(r) . \tag{20}$$

The cumulative two-point average of particles up to distance R, and the change in particles between distances or distance bands, are defined, respectively, as

$$\bar{N}(R) = \sum_{r=1}^{R} \bar{n}(r) , \tag{21}$$

and

$$\Delta\bar{N}(R) = \bar{N}(R) - \bar{N}(R-1) = \bar{n}(R) . \tag{22}$$

Density measures can now be formed, noting that the number of lattice points for each distance r is independent of the positions of k and l. In analogy to equation (15), the two-point cumulative density is given as

$$\bar{\rho}(R) = \frac{\bar{N}(R)}{S(R)} = \left[\sum_{r=1}^{R} \sum_{k=1}^{N} \sum_{l} p_{lk}(r) \right] \Big/ N \sum_{r=1}^{R} s(r) . \tag{23}$$

Density change can be computed as

$$\Delta\bar{\rho}(R) = \bar{\rho}(R) - \bar{\rho}(R-1) = \frac{\bar{N}(R)}{S(R)} - \frac{\bar{N}(R-1)}{S(R-1)} , \tag{24}$$

and the marginal change in density as

$$Q(R) = \frac{\Delta\bar{N}(R)}{\Delta S(R)} = \frac{\bar{n}(R)}{s(R)} = \frac{1}{N} \sum_{k=1}^{N} \left[\frac{\sum_{l} p_{lk}(r)}{s(r)} \right] . \tag{25}$$

As in the case of the one-point measures, the two-point measures in equations (21), (22), (23), and (25) will be used as approximations to equations (8) to (11) in that order.

The two-point measures clearly take account of any self-similarity in the physical structure, but in the case of all these measures, it is necessary to be extremely careful concerning the radial distances over which they are computed. Much of the subsequent analysis is concerned with these issues, for, in all cases, the measures are only appropriate for those parts of the system which are fully developed, and in any cluster this will be somewhat less than the total cluster itself. Lastly, Witten and Sander (1981; 1983) and Meakin (1983a; 1983b), amongst many who have worked with these models, argue that the two-point measures are considerably more appropriate than the one-point, and they suggest that the two-point density measure $\bar{Q}(R)$ is the best to use in estimating D. In the rest of this paper, we will use all the measures presented, thus demonstrating the sensitivity of the estimation to the measures themselves as well as to different ranges of distance.

5 Space-time histories and accounts

The DLA model has an extremely straightforward growth dynamics. Particles are launched one at a time and no more than one particle can be making a random walk on the lattice at any one point in time. Therefore a complete history of the system's growth dynamics is represented by the order in which the particles stick to the cluster along with their location on the lattice. We must now formulate the model with respect to time, t, as well as space, r, for several reasons. First, in comparison with real systems, it may be necessary to calibrate the model so that the theoretical process of growth can be tailored to an actual process if a development history of an urban area is available. Second, it is necessary to explore the stability of the cluster over time with respect to the stability of its dimension, D, and the spatial properties of successive particle locations. Third, and perhaps of greatest importance here, we need to measure the growth profiles

of the cluster with regard to its fully developed parts; thus the dynamics of the growth process will enable us to define the appropriate subcluster from the whole.

We will extend our spatial notation in which we refer to a distance by r, and everything up to a given distance by R, to an index of a particular time by t, and everything up to a given time by T. Assume that space is recorded by $r = 1, 2, \ldots, R_b$, where the units of space are distance bands and where R_b is the boundary of the system, and assume also that time is given by $t = 1, 2, \ldots, T_e$ where the units of time are periods and where T_e is the last (end) period in the growth process. Strictly speaking, each particle has a unique location in time and space, for no more than one lattice point is ever occupied and no more than one particle ever circulates in the system at any point in time. However, in the subsequent analysis, we require distance and time bands to be defined.

The basic unit of account is now the number of particles in distance band r and time period t, $\mathrm{n}(r, t)$. We are able to analyse this number over time or space or both. Thus

$$\mathrm{n}(t) = \sum_{r=1}^{R_b} \mathrm{n}(r, t) , \tag{26}$$

and

$$\mathrm{n}(r) = \sum_{t=1}^{T_e} \mathrm{n}(r, t) , \tag{27}$$

where $\mathrm{n}(r)$ is as defined in equation (12). Note that an equivalent unit of account $\bar{\mathrm{n}}(r, t)$ could be defined based on two-point averages, but this is less meaningful with respect to the actual growth of the cluster. Equations (26) and (27) when summed over t or r, respectively, add to give the total number of particles in the system, that is

$$N = \sum_{t=1}^{T_e} \mathrm{n}(t) = \sum_{r=1}^{R_b} \mathrm{n}(r) = \sum_{t=1}^{T_e} \sum_{r=1}^{R_b} \mathrm{n}(r, t) . \tag{28}$$

Equations (26) to (28) define a simple but complete set of space-time accounts.

It is necessary, however, to examine how the system converges towards the marginal and total sums in equations (26) to (28). Cumulative variables are thus defined as

$$\mathrm{N}(R, t) = \sum_{r=1}^{R} \mathrm{n}(r, t) , \tag{29}$$

and

$$\mathrm{n}(r, T) = \sum_{t=1}^{T} \mathrm{n}(r, t) . \tag{30}$$

Equations (29) and (30) are equal to (26) and (27) when $R = R_b$ and when $T = T_e$, respectively. A total accumulation over time and space, defined in analogy to equation (28), is

$$\mathrm{n}(R, T) = \sum_{t=1}^{T} \mathrm{n}(R, t) = \sum_{r=1}^{R} \mathrm{n}(r, T) = \sum_{t=1}^{T} \sum_{r=1}^{R} \mathrm{n}(r, t) . \tag{31}$$

The other variable of interest which serves to integrate these accounts with the previous one-point measures is defined as

$$\mathrm{N}(R) = \sum_{r=1}^{R} \mathrm{n}(r) = \sum_{t=1}^{T_e} \mathrm{n}(R, t) , \tag{32}$$

and the analogous cumulative total over time is given as

$$N(T) = \sum_{t=1}^{T} n(t) = \sum_{r=1}^{R_b} n(r, T) . \quad (33)$$

As $R \rightarrow R_b$ and $T \rightarrow T_e$, equations (32) and (33) converge to the total number of particles in the system, N, defined by equation (28).

For DLA simulations, we already have a clear idea how the growth process develops with respect to time and space, owing to the fact that, in general, particles launched later in time are added to tips of dendrites on the periphery of the cluster; in short, there is a strong correlation between time of launch and location of particles with respect to distance from the central seed in the cluster. Examining the distribution of particles $n(r, t)$ across space r for each time t, or across t for each distance band r, reveals wave-like phenomena with most particles locating in the latest time period on the edge of the cluster grown so far. The cumulative distributions $n(R, t)$ and $n(r, T)$ also show cumulative waves across space and time, as will be clearly illustrated in a later section when an example of the DLA model is presented. It is easy to show the buildup of waves of growth generated from $n(R, t)$, where R is accumulated over space but plotted at different times, t, and generated from $n(r, T)$, where T varies across time but is plotted for different distance bands r. We can also plot $n(R, T)$ through time but across space, and vice versa. In the rest of this paper, we will plot these variables on size–distance graphs for each individual time, t, and accumulated time, T, so that we can examine the spatial similarities through time and define appropriate thresholds for the one-point and two-point measurements of the cluster. But in future research we will have recourse to the complementary analysis plotted through time for different distance bands and accumulations thereof.

6 Theoretical simulations

6.1 *Statics*

Before we explore the statistical and spatial properties of a typical DLA simulation, we must present the method of simulation in more detail. As we indicated in an earlier section, a seed is first planted at a point on the lattice and a cluster is built up around this seed by launching particles at some distance far away from the edge of the cluster. Each particle makes a random walk on the lattice until it reaches a lattice point adjacent to one already occupied by a particle where it 'sticks', or until it leaves the system by crossing its boundary where it is deemed to have disappeared or have been destroyed. Although there is some debate about the anisotropy introduced by the geometry of the underlying lattice as we noted earlier, lattices based on a square grid have mainly been used and we will adopt this convention here.

To reduce the computation time required, particles are launched from a circular orbit which is set at the maximum radius of the cluster plus five lattice steps. Particles are deemed to have been destroyed once they enter the region outside the bounding circle which is set at least three times the maximum cluster radius. As the cluster builds up, its maximum radius, the launch circle, and the bounding circle increase continually, and with these conventions, clusters can be grown to any size: the only limits are computer time and memory. The geometry of the method is illustrated in figure 1(a) which shows how these assumptions are incorporated into the spatial development of the cluster. This mechanism, first proposed by Meakin (1983b), enables modest clusters of up to 10^4 or so particles to be grown in about ten hours CPU time using a MicroVax II minicomputer. However, if bigger clusters are required it is necessary to develop faster methods

However, if bigger clusters are required it is necessary to develop faster methods based on off-lattice random walks when the particle is far away from the cluster, with a transition to lattice walks in the neighbourhood of the cluster. Differences in form are not apparent and clusters of up to 10^5 particles have been grown successfully (Meakin, 1986b).

Here we will illustrate the operation of a typical DLA model but we must note that definitive results concerning the fractal dimension D of such models depend upon averaging the dimensions associated with many runs. Different clusters are produced for each run owing to the random walk mechanism of the model, and thus, on average, $D \approx 1.71 \pm 0.03$, where the value 0.03 represents the standard error (Jullien and Botet, 1987). This standard error is fairly low and suggests that, for the majority of runs, D should be within the range 1.68 to 1.74. The DLA simulation discussed here is shown in figure 1(b) where the grey tones give some idea of the sequence in which particles are added to the cluster. This aggregate consists of $N (= 10000)$ particles clustered around a seed particle which is located at the centre of a 500×500 square lattice.

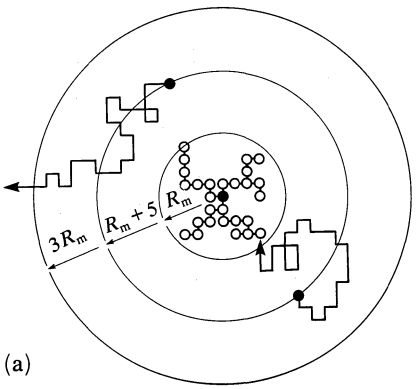

(a)

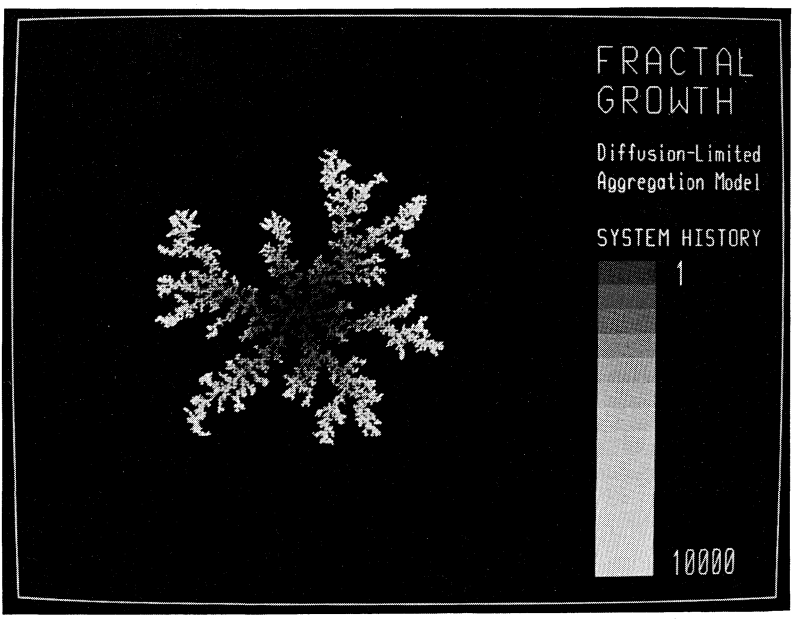

(b)

Figure 1. (a) The mechanism of diffusion-limited aggregation, and (b) fractal growth of on lattice diffusion-limited aggregation—a typical DLA simulation.

Some properties of this simulation are shown in table 1 which also includes similar properties of urban growth for the town of Taunton; these will be used later as a basis for comparison. To enable analysis to proceed, the various measures of cluster size and spread must be normalised with respect to the number of points in the lattice. Such normalisation involves the computing of indices relating to the size of the cluster and its radius. The maximum radius of the cluster, R_m, computed as the largest distance from any particle to the seed, can be used to compute the effective area of the cluster (πR_m^2) if all lattice points are occupied. The actual area is given by N (assuming each point occupies a unit square), thus the density here is only about 5% of the total effective area. This is an extremely sparse structure; indeed, all the occupied lattice points are on the boundary of the cluster and there are no interior points (occupied points entirely surrounded by other occupied points) whatsoever. The length of the boundary is 12.7 times the circumference ($2\pi R_m$) of the effective area, which represents a good measure of the tortuosity of the structure. The sparsity is also indicated by the fact that, on average, there are only about 2.4 nearest neighbours to each lattice point. We will return to this table in a later section when we come to examine the properties of the urban area making up the town of Taunton.

For both this DLA simulation and the subsequent application to Taunton, we will examine the spatial distribution of development by using the four relationships given earlier in equations (8) to (11). First, we use the one-point measures $N(R)$ from equation (13), $n(R)$ from equation (14), $\rho(R)$ from (16), and $Q(R)$ from (18) as approximations to $N(r)$, $dN(r)$, $\rho(r)$ and $dN(r)/dA(r)$ in equations (8) to (11) using fifty distance bands each of width $R_b/50$. The computed absolute values of these variables and their logarithmic transformations are shown in figures 2(a) and 2(b) (see over), respectively. Note that each distance band is the same width, thus an approximation to dr is not required in the analysis.

Table 1. Spatial properties of the theoretical and real systems.

System characteristics	DLA simulation	Taunton
Dimension of lattice	500 × 500	150 × 150
Lattice points	250000	22500
Points occupied, N	10000	3179
Maximum radius, R_m	248.24	62.94
Total effective area, πR_m^2	193601	12444
Average density, $N/\pi R_m^2$	0.052	0.256
Mean radius[a], $\overline{R}$	124.62	33.18
Standard deviation, σ	56.08	14.19
$\overline{R}/R_m$	0.502	0.527
σ/R_m	0.226	0.225
$\sigma/\overline{R}$	0.450	0.428
Length of boundary, B	19855	3994
Maximum circumference, $2\pi R_m$	1560.0	395.4
Tortuosity index, $B/2\pi R_m$	12.73	10.10
Number of boundary points, N_b	10000	2709
Density of boundary points, N_b/N	1.000	0.852
Interior points, N_i	0	470
Density of interior points, N_i/N	0	0.148
Nearest neighbours, N_n	23938	13804
Average neighbours, N_n/N	2.394	4.342

[a] Mean radius $\overline{R} = [\sum_i r_i \sum_l p_{fl}(r_i)]/N$, where r_i now represents the distance from the seed particle $k = 1$ to the distance band i which contains the particles l associated with r.

From equations (8) to (11), $N(r)$ should increase at an increasing rate, $dN(r)$ should increase at a decreasing rate, the density $\rho(r)$ should decrease at a decreasing rate, as should $dN(r)/dA(r)$. Figure 2(a) indicates this is so for $\rho(r)$ and $dN(r)/dA(r)$, but $N(r)$ behaves like a logistic function, and $dN(r)$ is almost parabolic. These functions should all be linear when plotted logarithmically, as in figure 2(b), but the graphs indicate very sharp changes in slope and direction in the neighbourhood of the radius $r \approx 125$ units. All this is an indication that the cluster is well developed up to this distance from the central seed; at greater distances the development is increasingly incomplete owing to the termination of the growth process. Thus it is standard practice in fitting these relationships to data to exclude longer distances which reflect the incomplete peripheral regions of the cluster, and sometimes to exclude short distances which can also be subject to volatile fluctuations in occupancy.

Therefore, we have generated the parameters from the following equations[1] which have been fitted using ordinary least-squares regression:

$$\left.\begin{aligned} \ln N(R) &= \alpha_1 + \beta_1 \ln(R/\text{units}) , \\ \ln n(R) &= \alpha_2 + \beta_2 \ln(R/\text{units}) , \\ \ln[\rho(R)/\text{units}] &= \alpha_3 + \beta_3 \ln(R/\text{units}) , \\ \ln[Q(R)/\text{units}] &= \alpha_4 + \beta_4 \ln(R/\text{units}) . \end{aligned}\right\} \tag{34}$$

Initially, we fitted these equations to all fifty distance bands, then reestimated their parameters using an upper cutoff after the twenty-sixth band, and produced a final estimation of the equations excluding the first three distance bands. These thresholds/cutoffs are indicated in figure 2.

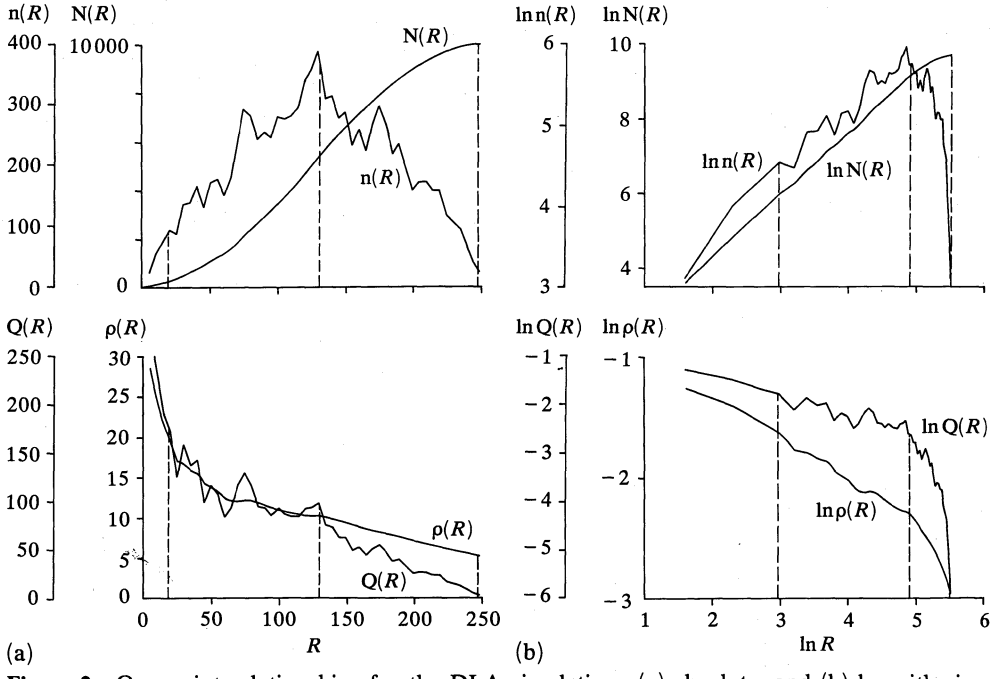

Figure 2. One-point relationships for the DLA simulation: (a) absolute, and (b) logarithmic.

[1] In these equations, the word 'units' applies to the parameter immediately preceding it. Thus if $\rho(R)$ is measured in units of m^{-3} then it is divided by these units to leave a pure number of which the natural logarithm is taken.

Estimates of the various parameters β_1, β_2, β_3, and β_4 are shown in table 2(a), with their standard errors in table 2(b), and their adjusted R^2-values[2] in table 2(c). For these one-point estimates, β_1 and β_3 are related by: $\beta_3 = \beta_1 - 2$, and thus there are only three, not four, independent estimates in these tables. The initial estimation over all fifty distance bands reveals volatile R^2-values and considerable inconsistency between the β estimates. Note that we have computed the fractal dimension D from these β parameters and these are also shown in table 2(a). Cutting off the cluster at the twenty-sixth band improves these results dramatically. The standard errors are considerably lower and all R^2-values are greater than 0.850. The fractal dimension of 1.665 from β_1 is close to the value of 1.71 produced in averaging many DLA simiulations, and it is even closer to Muthukumar's (1983) field theory prediction that $(d^2+1)/(d+1) = 1.666$. Excluding the range of shorter distances does not change these estimates very much, and it is encouraging that all three independent estimates of D from β_1, β_2, and β_4 for distance ranges 1-26 and 4-26 lie between 1.638 and 1.777.

It is widely argued in the literature that two-point measures are considerably better than one-point, for these measures capture the dilation symmetry or self-similarity implicit in figure 1(b). Using $\bar{N}(R)$, $\tilde{n}(R)$, $\tilde{\rho}(R)$, and $\bar{Q}(R)$ from equations (21), (22), (23), and (25), respectively, as the dependent variables in equations (34) provides us with another set of estimates of the fractal dimension D. First these variables are plotted against distance in absolute and logarithmic form, as shown in figure 3 (see over). The graphs are considerably smoother than those in figure 2 owing to the extensive averaging for every particle related to every other. In fact the two-point averages require about three hours CPU time on a MicroVax II and these cannot easily be generated alongside the DLA simulation. Moreover, the set of distances now relates to all possible distances between every lattice point, there being a total of R (= 1, 2, ... , 488) in contrast to the one-point measures where we have assumed that fifty distance bands is a good approximation to the variation in the cluster up to $R_b = 248$. It is considerably more difficult to detect distance thresholds from these plots because of their smoothness. Thus we have selected five possible ranges for estimation purposes. The initial range uses all 488

Table 2. One-point estimates of the scaling equations for the DLA simulation.

Distance bands	$\beta_1 = D$	$\beta_2 = D-1$	$\beta_3 = D-2$	$\beta_4 = D-2$
(a) β-coefficients and fractal dimensions (in brackets)				
1-50	1.574	0.267	−0.426	−0.826
	(1.574)	(1.267)	(1.574)	(1.174)
1-26	1.665	0.777	−0.335	−0.362
	(1.665)	(1.777)	(1.665)	(1.638)
4-26	1.659	0.739	−0.340	−0.314
	(1.659)	(1.739)	(1.659)	(1.686)
(b) Standard errors of β-coefficients				
1-50	0.017	0.100	0.017	0.095
1-26	0.006	0.032	0.006	0.029
4-26	0.009	0.049	0.009	0.050
(c) Adjusted R^2-statistics				
1-50	0.994	0.111	0.924	0.602
1-26	1.000	0.959	0.992	0.856
4-26	0.999	0.908	0.985	0.632

[2] 'R^2-value' always refers to the statistic R^2, *not* to the distance R^D.

distances, but this is reduced to 174, 11-174, 11-157, and 11-123, the last three also excluding the first ten bands.

Estimates of the β parameters and the associated fractal dimensions are shown in table 3(a). As expected, these coefficients are quite inconsistent when estimated

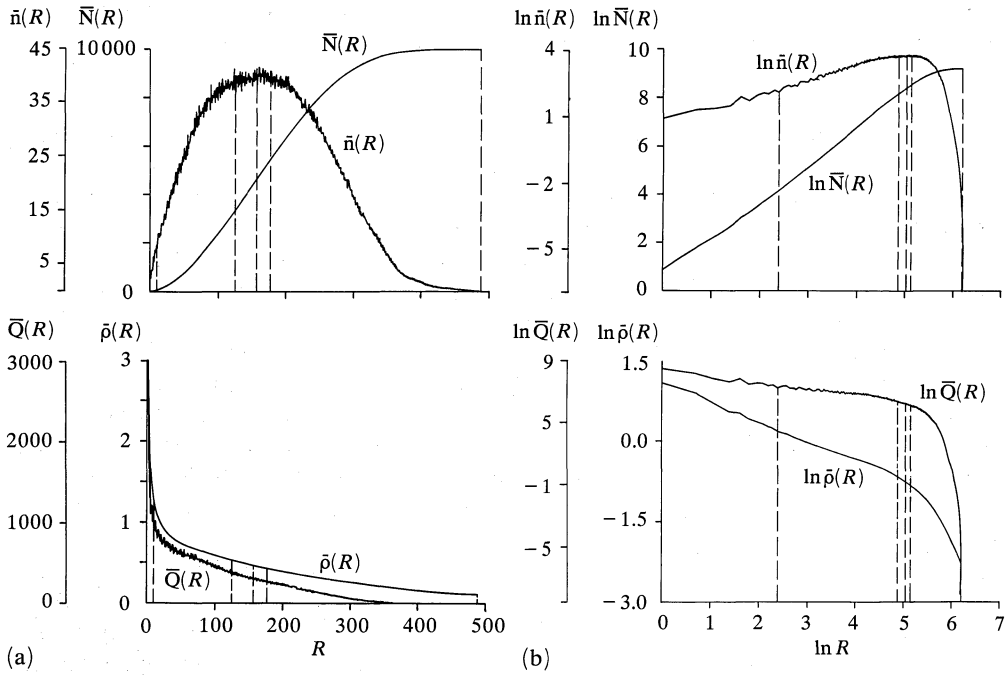

Figure 3. Two-point relationships for the DLA simulation: (a) absolute, and (b) logarithmic.

Table 3. Two-point estimates of the scaling equations for the DLA simulation.

Distance bands	$\beta_1 = D$	$\beta_2 = D-1$	$\beta_3 = D-2$	$\beta_4 = D-2$
(a) β-coefficients and fractal dimensions (in brackets)				
1-488	1.338	−0.839	−0.633	−1.821
	(1.338)	(0.161)	(1.367)	(0.179)
1-174	1.586	0.588	−0.356	−0.412
	(1.586)	(1.588)	(1.644)	(1.588)
11-174	1.619	0.545	−0.359	−0.455
	(1.619)	(1.545)	(1.641)	(1.545)
11-157	1.631	0.575	−0.346	−0.425
	(1.631)	(1.575)	(1.654)	(1.575)
11-123	1.652	0.640	−0.323	−0.359
	(1.652)	(1.640)	(1.677)	(1.641)
(b) Standard errors of β-coefficients				
1-488	0.011	0.081	0.012	0.079
1-174	0.004	0.008	0.002	0.008
11-174	0.003	0.011	0.004	0.011
11-157	0.003	0.010	0.003	0.010
11-123	0.002	0.009	0.002	0.009
(c) Adjusted R^2-statistics				
1-488	0.966	0.178	0.852	0.519
1-174	0.999	0.972	0.992	0.945
11-174	0.999	0.941	0.983	0.917
11-157	1.000	0.954	0.988	0.920
11-123	1.000	0.978	0.997	0.933

over the whole range of distances, but as the ranges are reduced, the coefficients converge quite remarkably, to give fractal dimensions between 1.640 and 1.677. The standard errors shown in table 3(b) and the correlations in table 3(c) are also much improved as the range is reduced, with the final estimates based on the range 11 - 123 giving near perfect correlations. From the analysis, it would appear that the fractal dimension is nearer 1.66 than 1.71, and this is borne out in several other simulations we have generated. However, we have not attempted anything like the number of simulations reported by Witten and Sander (1983) and Meakin (1983b), amongst others, although it is interesting that over the seven years since the DLA model was proposed, the certainty with which researchers have held to the universality of $D \approx 1.71$, has become much weaker. The precise value of D, however, whether it be 1.66 or 1.71 is not important here. What is important is that DLA generates self-similar forms which provide a baseline for comparison with real growth, and it also provides a vehicle for adapting such models to more realistic simulations of urban growth and form.

6.2 *Dynamics*

As already indicated, we will not examine the temporal dynamics in the DLA model in all their detail, for we do not have a real history of urban growth on which to base our comparisons. But we are able to use the model dynamics to explore the extent to which the cluster is complete at any stage of its development. This issue has already been broached in selecting distance thresholds for the estimation of fractal dimensions, as reported above.

There are two aspects of the growth process which we will focus upon: first, the question of spatial development with respect to the form of the cluster, and, second, measurement of the statistical properties of the cluster at different time periods. We have arbitrarily divided the growth process into $10(= T_e)$ time periods and have allocated $1000(= N/T_e)$ particles to each time period. In short, we will associate the first 1000 particles with $t = 1$, the second thousand with $t = 2$, and so on. With respect to the temporal accounts presented earlier, for each time period t

$$\mathrm{n}(t) = \sum_{r=1}^{R_b} \mathrm{n}(r, t) = 1000 , \tag{35}$$

and

$$N = \sum_{t=1}^{T_e} \sum_{r=1}^{R_b} \mathrm{n}(r, t) = \sum_{t=1}^{T_e} \mathrm{n}(t) = 10000 . \tag{36}$$

The location of each of the N particles on the lattice with respect to each time period t in which the location takes place, is shown in figure 4 (see over). This is a dramatic example of the model's growth dynamics which indicates quite clearly how the ultimate form of the cluster is established. The first and perhaps second time periods determine the basic skeleton of the form, with subsequent evolution largely representing the addition of particles to the already established dendrites. Growth takes place mainly on the cluster tips. We have computed the correlation (R^2) between the location of particles represented in terms of the radial distance from the seed and the time of development: this R^2-value is 0.79 for a linear comparison and it rises to 0.90 if a nonlinear relationship between time and space is postulated. These are very high values, giving a clear indication that the dendritic structure is extremely effective in screening undeveloped areas from further development. Figure 4 also presents a classic example of the fact that the overall form of the cluster cannot easily be inferred from its parts. Finally, that the underlying lattice on which the cluster is based introduces anisotropy, which biases the form to a diamond shape (Meakin, 1986c), is seen clearly in the growth of the cluster in later time periods.

The wavelike spread of the cluster is clearly observed in figure 4, but the high correlation between space and time must be qualified in that some particles are still locating at short distances from the seed as late as the final time period. For example, in the fifth time period, particles are locating in the eleventh distance band from the centre whereas in the last (tenth) time period, particles are locating as close in as the eighteenth distance band when over 90% of the cluster has already been developed. It is these effects that make it essential to consider a fairly tight distance threshold over which to measure the cluster's properties, as was used in the previous section.

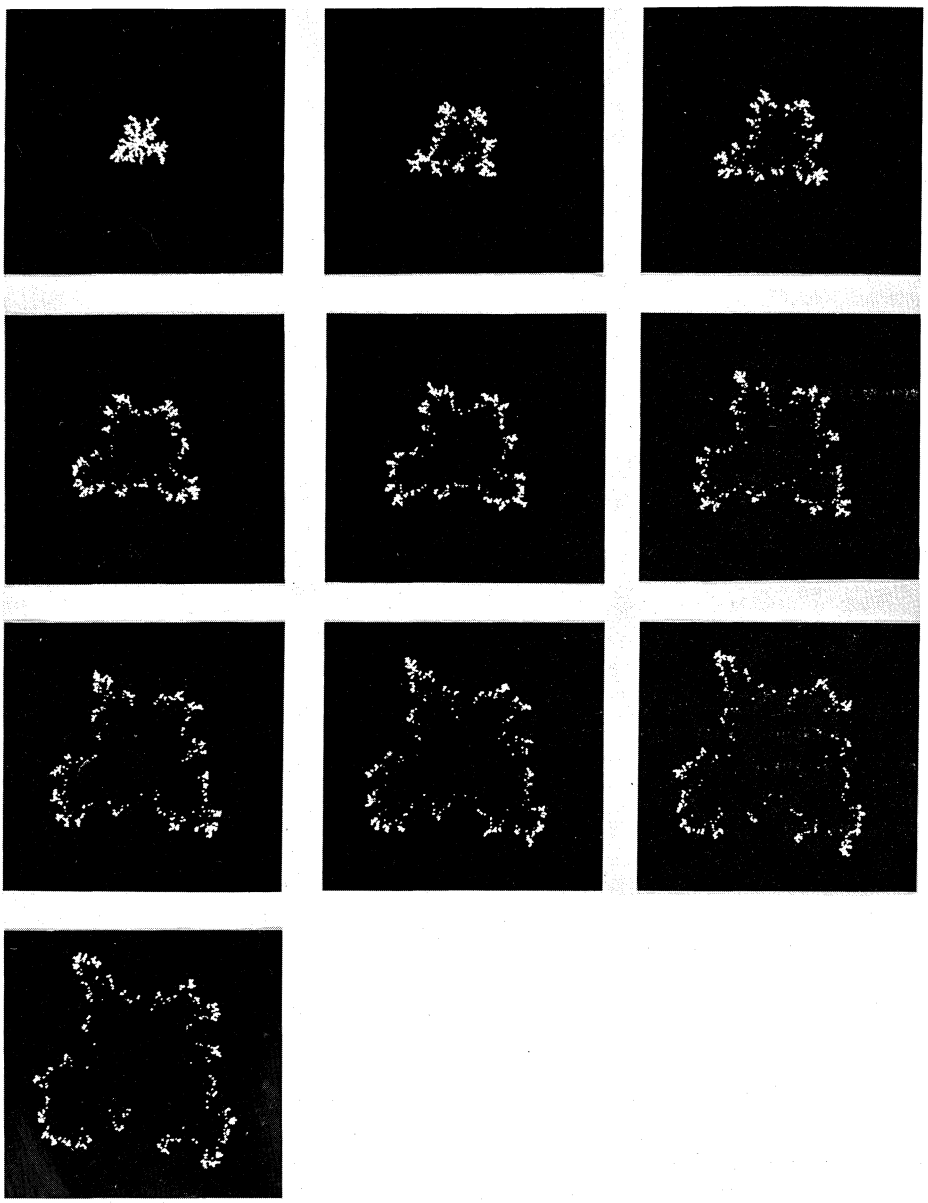

Figure 4. Spatial dynamics of the DLA simulation.

It is also possible to demonstrate the wavelike growth of the system in a manner akin to the cumulative and individual growth of population, given by N(R) and n(R), respectively. In figure 5, we have graphed the cumulative total n(R, t) for increasing R in terms of each of the ten time periods. This is essentially the growth pictured in figure 4 collapsed to one-dimensional form. The individual profiles, n(r, t), are also graphed and these show the overlapping nature of the waves which occur when all the particles in figure 4 are collapsed to form figure 1(b). Figure 5 also shows the cumulative total n(R, T) over R for cumulative time T = 1, 2, ... Note that the graph of n(R, T_c) is that of N(R) shown in figure 2(a). The composition of the aggregate of individual change n(R), given as n(r, T) where T = 1, 2, ... , is also shown, revealing how wave upon wave of growth builds up the overall cluster.

We can also estimate the stability of the cluster through time by computing the fractal dimension associated with n(R, t) and n(R, T) in figure 5, using the graphs of n(R, t) and n(R, T) to indicate appropriate distance thresholds over which the regressions can be run. Both these variables n(R, t) and n(R, T) should be proportional to R^D if the cluster is fractal in its parts. Appropriate distance thresholds have been set by inspecting changes in the profiles of n(R, t) and n(R, T) in figure 5. The fractal dimensions associated with these cumulative populations are shown in figure 6 (see over). For n(R, t), the fractal dimensions are fairly volatile ranging from 1.351 to 1.966, with R^2-values ranging from 0.950 to 0.999. When these same regressions are carried out on the cumulative population which is also accumulating over time periods n(R, T) the dimensions estimated are much more characteristic of the dimensions given in tables 2(a) and 3(a). These dimensions vary from 1.600 to 1.664, with the dimension falling slightly in later time periods. The R^2-values only vary from 0.997 to 0.999. What is important for analysis is the great variation in fractal dimension of the accumulation that is

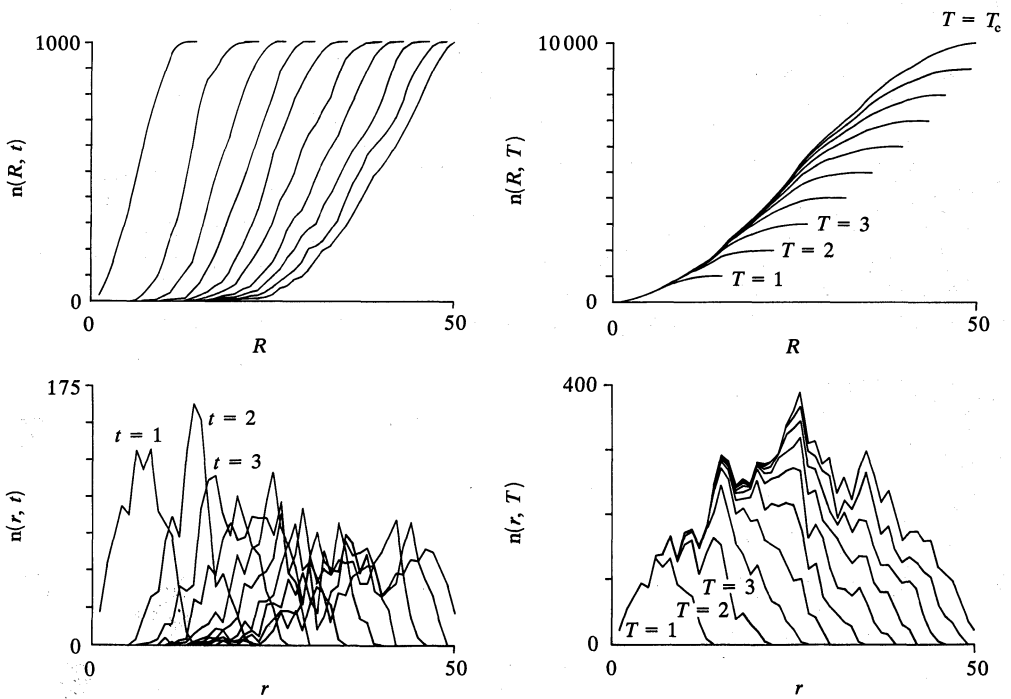

Figure 5. Diffusion waves characterising the DLA simulation.

time period specific. Whereas the first time-period development shown in figure 4 looks fractal with $D = 1.664$, later ones do not. Remarkably, though, once put together to form the whole cluster as shown in figure 1(b), these patterns appear fractal over many scales: an intriguing demonstration that the whole is greater than the sum of the parts.

This type of analysis is of considerable significance for any adaptation of the model which might attempt to incorporate some reversibility. The early development of the cluster appears to have an enormous influence on the ultimate form, and it is this early development which would be the first to be subject to further change. If these earlier parts of the cluster were to change, the whole cluster might suddenly become nonfractal in form. Indeed, this type of experiment is worth attempting without thinking of any reversible DLA process so that the dependence of the overall cluster on its parts can be explored more thoroughly: an important matter for further research.

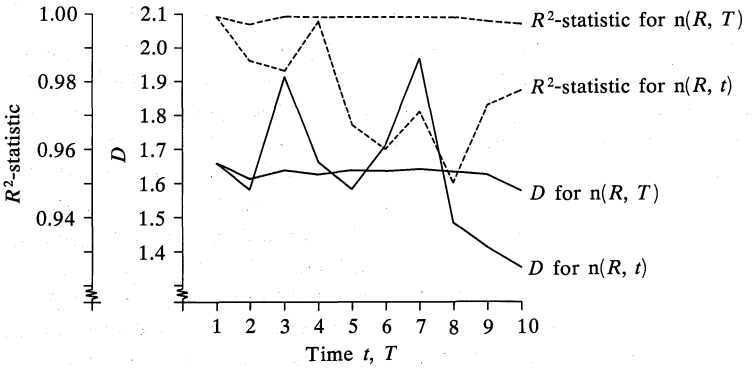

Figure 6. Time-dependent fractal dimensions and correlation coefficients (R^2) for the evolving DLA cluster.

7 Empirical applications: the urban growth of Taunton

To develop DLA and related models of urban systems it is first essential to see how close the baseline model is to reality. One of the features of our model is that the final form of system which it generates does not account for any specific constraints on its development other than those posed by the geometry of the dendrites which screen areas from further growth. Accordingly, we have selected an urban area whose development has not been strongly affected by its underlying geomorphology or by large-scale man-made constraints. We chose the town of Taunton in Somerset, South West England (population about 49000 in 1981) which met these criteria quite well and also provided a manageable digitising task.

The urban form was digitised on a 50 m grid imposed on the 1:10000 scale Ordnance Survey maps which were last revised in 1981. This scale was not fine enough to pick up individual locations but it was sufficient as a first attempt in that it involved making hard decisions about the exclusions of small areas of open space and, of course, nonpopulation-related land-uses. It is clear, however, that the underlying form of the population distribution in detailed spatial terms is still largely unknown, although detailed scrutiny of the 1:10000 scale does reveal considerably greater variety in geometry than has been picked up in the measurements illustrated here.

The digitised map of urban Taunton is shown in figure 7. Although this does not reveal a clear dendritic structure, this is as much owing to the scale of digitisation as to the fact that no dendritic structure might exist. There are 3179

developed cells in this form, which are contained within a rectangular grid of 110×118 cells. These cells were then located on a square 150×150 lattice with the centre positioned on the ruined castle, the first known centre of settlement. The physical characteristics of the town have been given previously in table 1 where direct comparisons can be made with the DLA simulation. The density of cells or lattice points is much higher than the DLA simulation: nearly 26% of all points in the total effective area are occupied, in contrast to only 5% in the DLA simulation. However, it is remarkable that 85% of the 3179 cell points are on the boundary, only 15% being classed as interior points. The index of tortuosity is 10.100 in comparison to 12.729 for the DLA simulation, but there are nearly twice as many nearest neighbours for each occupied point in Taunton in comparison with the DLA example (4.342 compared with 2.394). One fascinating similarity involves the mean radius, $\overline{R}$, which is 52% of the maximum radius in Taunton, 50% in the DLA, and the ratio of the standard deviation to this mean is 0.225 in both cases. Although Taunton is more compact than the DLA cluster, several of its basic dimensions are comparable, as table 1 shows.

Measurement of the four relationships given in equations (8) to (11) proceeded in the same way for Taunton as in the DLA simulation. The measures $N(R)$, $n(R)$, $\rho(R)$, and $Q(R)$ were computed and graphed over fifty distance bands as shown in figure 8(a). Figure 8(b) illustrates their logarithmic transformation, and a comparison of figures 8(a) and 8(b) with figures 2(a) and 2(b), respectively, for the DLA simulation reveals a strong similarity. The major difference is the clear discontinuity in these relations within short distances of the centre of the town, which is strong evidence of reversibility in that it is consistent with the crater effect observed in population profiles around the central business district in many Western cities. This is clearly seen in the density variables $\rho(R)$ and $Q(R)$ and their logarithmic transformation in figure 8.

In estimating the parameters of equations (34) by using the Taunton data, the need to restrict the distance range by defining cutoff points is also clear from these figures. We have defined four ranges beginning with all fifty distance bands,

Figure 7. Urban development in Taunton at 1981 digitised from 1:10000 Ordnance Survey map.

restricting these to the first thirty-four, then excluding the first six bands and finally the first eight. The β parameters and fractal dimensions are given in table 4(a). There is considerably more volatility in these estimates than in the case of DLA, with probably the best results reflected in the narrower ranges 6-34 and 8-34. Fractal dimensions vary between 1.573 and 1.716 for the 6-34 range and between 1.484 and 1.647 for the 8-34 range. Standard errors in table 4(b) and R^2-statistics in table 4(c) are also more variable than for the DLA model, but there

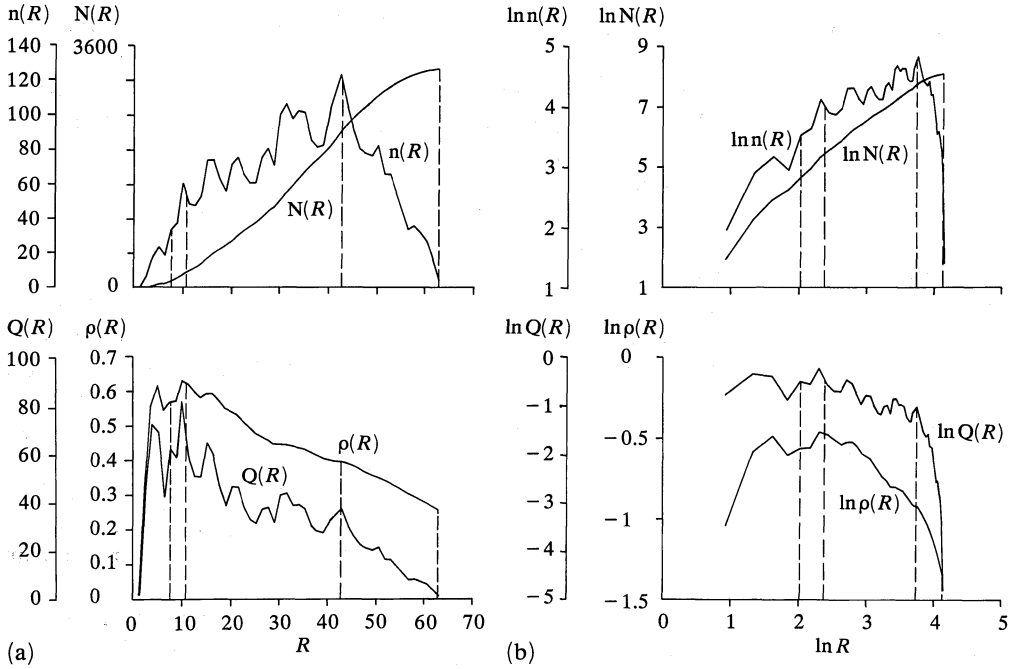

Figure 8. One-point relationships for Taunton: (a) absolute, and (b) logarithmic.

Table 4. One-point estimates of the scaling equations for Taunton.

Distance bands	$\beta_1 = D$	$\beta_2 = D-1$	$\beta_3 = D-2$	$\beta_4 = D-2$
(a) β-coefficients and fractal dimensions (in brackets)				
1-50	1.766	0.309	−0.234	−0.746
	(1.766)	(1.309)	(1.766)	(1.254)
1-34	1.893	0.787	−0.107	−0.283
	(1.893)	(1.787)	(1.893)	(1.727)
6-34	1.716	0.573	−0.284	−0.464
	(1.716)	(1.573)	(1.716)	(1.536)
8-34	1.647	0.515	−0.353	−0.516
	(1.647)	(1.515)	(1.647)	(1.484)
(b) Standard errors of β-coefficients				
1-50	0.032	0.121	0.032	0.118
1-34	0.034	0.051	0.034	0.047
6-34	0.022	0.057	0.022	0.056
8-34	0.013	0.069	0.013	0.069
(c) Adjusted R^2-statistics				
1-50	0.984	0.104	0.522	0.446
1-34	0.990	0.882	0.217	0.523
6-34	0.996	0.784	0.861	0.703
8-34	0.998	0.680	0.967	0.678

is some evidence here that the dimension D is a little lower than for the DLA simulation, notwithstanding the fact that the town is more compact.

Measurement of the two-point variables also proceeded in the same manner as that reported earlier. The graphs of $\bar{N}(R)$, $\bar{n}(R)$, $\bar{\rho}(R)$, and $\bar{Q}(R)$ against distance, shown as absolutes and logarithmic transformations in figure 9, are again very similar to those for the DLA simulation as shown in figure 3. These graphs are smoother than the one-point measures and they do not show any crater effect at

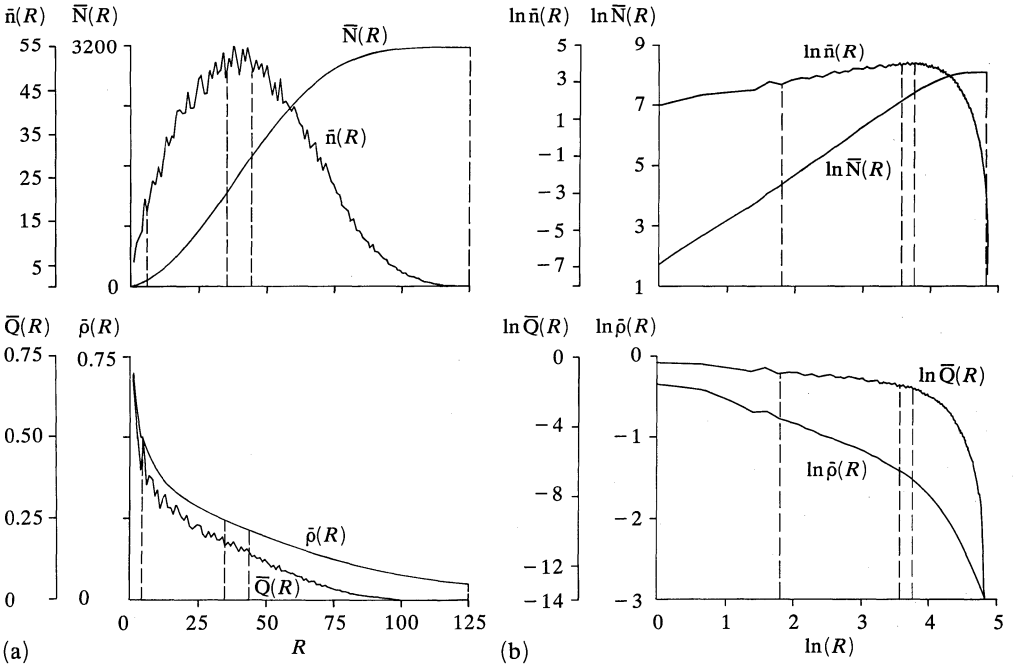

Figure 9. Two-point relationships for Taunton: (a) absolute, and (b) logarithmic.

Table 5. Two-point estimates of the scaling equations for Taunton.

Distance bands	$\beta_1 = D$	$\beta_2 = D-1$	$\beta_3 = D-2$	$\beta_4 = D-2$
(a) β-coefficients and fractal dimensions (in brackets)				
1-125	1.284	−0.983	−0.647	−1.979
	(1.284)	(0.017)	(1.353)	(0.021)
1-43	1.539	0.584	−0.337	−0.416
	(1.539)	(1.584)	(1.663)	(1.584)
6-43	1.588	0.525	−0.384	−0.474
	(1.588)	(1.525)	(1.616)	(1.526)
6-35	1.574	0.570	−0.362	−0.429
	(1.574)	(1.570)	(1.638)	(1.571)
(b) Standard errors of the β-coefficients				
1-125	0.022	0.181	0.025	0.179
1-43	0.005	0.015	0.007	0.015
6-43	0.005	0.022	0.006	0.022
6-35	0.004	0.025	0.005	0.025
(c) Adjusted R^2-statistics				
1-125	0.964	0.187	0.843	0.494
1-43	1.000	0.972	0.981	0.947
6-43	1.000	0.941	0.989	0.929
6-35	1.000	0.948	0.993	0.912

small distances within the density profiles. In some respects, the distance thresholds are easier to define than for the one-point measures. We begin with all 125 distances, reduce these to the first 43, cut out the first 5 values, and finally work with the range 6–35. The β parameters and fractal dimensions are shown in table 5(a). In contrast to table 4(a), the fractal dimensions increase in value as the ranges are restricted, the best values being those in the 6–35 range where D varies between 1.570 and 1.638. The standard errors in table 5(b) are better than those for the one-point averages as are the R^2-statistics shown in table 5(c). In fact, the values in the ranges 1–43 and 6–43 are not radically different from those in the 6–35 range, and as in the one-point analysis the fractal dimensions would appear to be lower than those for the DLA simulation.

What is clear from this analysis is that urban density in Taunton is associated with a more compact urban form than that produced by DLA. Growth in Taunton is structured around four or five main tentacles emanating from the centre, which is fairly similar to the DLA simulation. But the fingers of growth are much wider in Taunton, and it is not possible to say anything about self-similarity in this example because of the level at which urban growth was digitised. Nevertheless, this analysis is suggestive and encouraging enough to prompt us to search further and to develop finer measurement techniques for revealing the geometry of urban form.

8 Conclusions: directions for further research

We could have chosen other particle simulation models which give more compact clusters than the DLA model. There are a number of variants which are being actively explored based not only upon particle–cluster aggregation, but cluster–cluster aggregation, ballistic aggregation, percolation, and so on. In fact, there are different ways of formulating the DLA model in terms of probability fields, which involve rather different methods of simulation. Nittmann and Stanley (1986), for example, developed models governed by parameters that explicitly control the compactness of the resulting form, in which dendritic forms can be simulated as particular cases.

There are several extensions to our baseline model which have already been developed (Jullien and Botet, 1987). Lowering the sticking probabilities can increase the compactness, and constraints on the direction of the random walk have a strong influence on the resulting form. Many of these forms are not fractal but there is increasing doubt that the Witten–Sander DLA model is fractal over as many orders of scale as has been assumed, and recently large-scale off-lattice simulations suggest the existence of somewhat different forms (Meakin, 1986c). In any case, the concept of fractal dimension itself should not be interpreted too narrowly. Strictly speaking, this dimension only exists as a mathematical limit (Feder, 1988), and its real importance is in the identification of appropriate length scales and self-similarities which provide useful but contingent characterisations that are dependent upon context.

A related use of the DLA model as a baseline for urban simulation involves the focus upon urban form. The geometry of urban form has largely remained separate from empirical and theoretical models of urban structure. In the case of discrete urban models, form is represented as areas defined by points or centroids, whereas in urban density theory, form is largely assumed away in assumptions concerning monocentricity. Consequently, in the measurement of urban densities there has been little thought given to the underlying geometry of urban structure. Our focus on fractal models changes this substantially. Very hard questions about the space which individuals occupy have to be resolved, as inappropriate definitions of density will hinder the development of any models in which growth processes

and geometrical form are inextricably linked. In future work, we need to look at the underlying patterns of urban growth, and this will involve the collection of new data and the visualisation of the old in new ways. Moreover, this emphasis will involve a discussion as to whether urban density should be conceived in two or three dimensions, noting of course that DLA models can easily be extended to three or more dimensions (Meakin, 1983b).

The DLA model is one of the simplest formulations of irreversible cluster growth. We know that the assumption of irreversibility (that is, that once particles stick, they never move) is incorrect with respect to urban structure. Densities of large cities increase over time, whereas growth by DLA leads to lower average densities as the aggregate grows. The difference is largely accountable in terms of reversibility as seen in the fall in central city densities and the flattening of density gradients over time (Bussière, 1972; Parr, 1985). There is little work as yet on DLA models that incorporate reversibility, but extending such models is not difficult in principle, given that a complete history of particle aggregation is always available. The real issue is to extend such models in ways which appear close to what we know about urban growth and decline without losing the underlying simplicity in their growth processes and the resulting geometry. But first we need better models and better data, or at least data and models which are closer to each other.

In conclusion then, we see the value of this work not in any argument about whether or not urban form is fractal but in developing models which link urban growth and development to form much more clearly. To this end, the scaling relationships which characterise the extent to which activities in cities fill space are central, and if robust relationships between form and process can be established, it may then be possible to assess and perhaps devise policy instruments which direct urban growth and form in acceptable ways.

Acknowledgements. We wish to thank Hilary Crossweller who digitised the map of Taunton, Nathan Webster for photography, Tracey Wiltshire for cartographic work, and Beryl Collins who typed the manuscript.

References

Bertuglia C S, Leonardi G, Occelli S, Rabino G A, Tadei R, Wilson A G (Eds), 1987 *Urban Systems: Contemporary Approaches to Modelling* (Croom Helm, Andover, Hants)

Bussière R (Ed.), 1972 *Modèles Mathématiques de Répartition des Populations Urbaines* (Centre de Recherche d'Urbanisme, Paris)

Curry L, 1972, "A spatial analysis of gravity flows" *Regional Studies* **6** 131 - 147

Dutton G, 1973, "Criteria of growth in urban systems" *Ekistics* **215** 298 - 306

Feder J, 1988 *Fractals* (Plenum Press, New York)

Forrest S R, Witten T A, 1979, "Long-range correlations in smoke-particle aggregates" *Journal of Physics A* **12** L109 - L117

Jullien R, Botet R, 1987 *Aggregation and Fractal Aggregates* (World Scientific Publishing Company, Singapore)

Kadanoff L P, 1986, "Fractals: where's the physics?" *Physics Today* **39**(2) 6 - 7

Lovejoy S, Schertzer D, Ladoy P, 1986, "Fractal characterization of inhomogeneous geophysical measuring networks" *Nature (London)* **319** 43 - 44

Mandelbrot B B, 1983 *The Fractal Geometry of Nature* (W H Freeman, San Francisco, CA)

Meakin P, 1983a, "Diffusion-controlled cluster formation in two, three and four dimensions" *Physical Review A* **27** 604 - 607

Meakin P, 1983b, "Diffusion-controlled cluster formation in 2 - 6 dimensional space" *Physical Review A* **27** 1495 - 1507

Meakin P, 1985, "The structure of two-dimensional Witten - Sander aggregates" *Journal of Physics A* **18** L661 - L666

Meakin P, 1986a, "Some recent advances in the simulation of diffusion-limited aggregation and related processes", in *Fractals in Physics* Eds L Pietronero, E Tosatti (North-Holland, Amsterdam) pp 205 - 212

Meakin P, 1986b, "Computer simulation of growth and aggregation processes", in *On Growth and Form: Fractal and Non-fractal Patterns in Physics* Eds H E Stanley, N Ostrowsky (Martinus Nijhoff, The Hague) pp 111-135

Meakin P, 1986c, "Universality, non-universality and the effects of anisotropy on diffusion-limited aggregation" *Physical Review A* **33** 3371-3382

Mills E S, 1970, "Urban density functions" *Urban Studies* **7** 5-20

Muthukumar M, 1983, "Mean-field theory for diffusion-limited cluster formation" *Physical Review Letters* **50** 839-842

Niemeyer L, Pietronero L, Wiesmann H J, 1984, "Fractal dimension of dielectric breakdown" *Physical Review Letters* **52** 1033-1036

Nittmann J, Daccord G, Stanley H E, 1985, "Fractal growth of viscous fingers: quantitative characterization of a fluid instability phenomenon" *Nature (London)* **314** 141-144

Nittmann J, Stanley H E, 1986, "Tip splitting without interfacial tension and dendritic growth patterns arising from molecular anisotropy" *Nature (London)* **321** 663-668

Nordbeck S, 1971, "Urban allometric growth" *Geografiska Annaler* **53B** 54-67

Parr J B, 1985, "A population density approach to regional spatial structure" *Urban Studies* **22** 289-303

Sander L M, 1987, "Fractal growth" *Scientific American* **256** 82-88

Satpathy S, 1986, "Dielectric breakdown in three dimensions", in *Fractals in Physics* Eds L Pietronero, E Tosatti (North-Holland, Amsterdam) pp 173-176

Stanley H E, Ostrowsky N (Eds), 1986 *On Growth and Form: Fractal and Non-fractal Patterns in Physics* (Martinus Nijhoff, The Hague)

Stewart J Q, Warntz W, 1958, "Physics of population distribution" *Journal of Regional Science* **1** 99-123

Thrall G I, 1987 *Land Use and Urban Form* (Methuen, Andover, Hants)

Turkevich L A, Scher H, 1985, "Occupancy-probability scaling in diffusion-limited aggregation" *Physical Review Letters* **55** 1026-1029

Wilson A G, 1969, "The use of analogies in geography" *Geographical Analysis* **1** 225-233

Witten T A, Sander L M, 1981, "Diffusion-limited aggregation, a kinetic critical phenomenon" *Physical Review Letters* **47** 1400-1403

Witten T A, Sander L M, 1983, "Diffusion-limited aggregation" *Physical Review B* **27** 5686-5697

Woldenburg M J, 1973, "An allometric analysis of urban land use in the United States" *Ekistics* **215** 282-290

Woolley B, 1988, "In search of a postmodern maths" *The Guardian* 10 June, page 29